Journal of
Materials Chemistry C

CORRECTION

View Article Online
View Journal | View Issue

Cite this: *J. Mater. Chem. C*, 2025, **13**, 10434

DOI: 10.1039/d5tc90066b

rsc.li/materials-c

Correction: Bimetal-decorated resistive gas sensors: a review

Ka Yoon Shin,[a] Yujin Kim,[b] Ali Mirzaei,*[c] Hyoun Woo Kim*[a] and Sang Sub Kim*[b]

Correction for 'Bimetal-decorated resistive gas sensors: a review' by Ka Yoon Shin *et al.*, *J. Mater. Chem. C*, 2025, **https://doi.org/10.1039/D5TC00145E**.

The authors sincerely regret that in the published article, in eqn (3) the "+" symbol was omitted on the left side, and a previous version of Fig. 5 was inadvertently used; in addition, the final two paragraphs from section 3, "Bimetal-decorated resistive gas sensors", Tables 2 and 3, and the Author contributions section, were omitted from the final published article. These details correspond to the revised manuscript that was approved for publication during the peer review process.

The correct form of eqn (3) is as follows:

$$O_2^-(ads) + e^- \rightarrow 2O^-(ads) \tag{3}$$

The correct version of Fig. 5 is as follows:

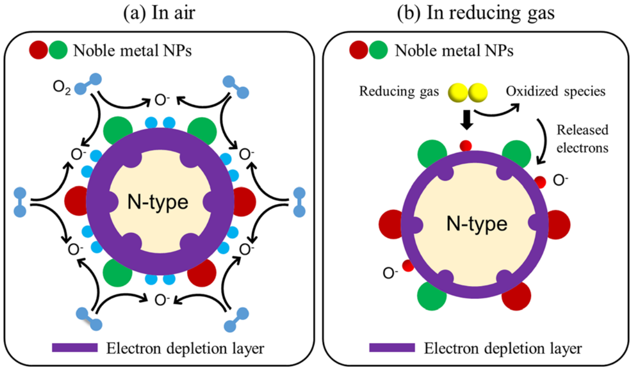

Fig. 5 (a) and (b) Catalytic effect of noble metals for enhanced gas response of resistive gas sensors.

The omitted paragraphs, and Tables 2 and 3, should appear immediately before the heading "Conclusions and outlook", and should read as follows:

Table 2 summarizes the gas sensing performance of various bimetal-decorated resistive gas sensors. Overall, bimetal-decorated gas sensors have been successfully used for the detection of various gases such as H_2, NO_2, C_3H_6O, H_2S, CH_4, and CO gases. The optimal sensing temperature varies between RT to 400 °C depending on gas type, type of sensing material and type of bimetallic system. Response and recovery times also mainly depend on the sensing temperature; however, they are often short. Bimetal-decorated gas sensors generally have good long-term stability and show good stability at least up to 30 days after fabrication.

[a] Division of Materials Science and Engineering, Hanyang University, Seoul 04763, Republic of Korea. E-mail: hyounwoo@hanyang.ac.kr
[b] Department of Materials Science and Engineering, Inha University, Incheon 22212, Republic of Korea. E-mail: sangsub@inha.ac.kr
[c] Department of Materials Science and Engineering, Shiraz University of Technology, Shiraz 715557-13876, Islamic Republic of Iran. E-mail: mirzaei@sutech.ac.ir

Table 2 Summary of gas sensing performance of various bimetal-decorated resistive gas sensors

Sensing material	Gas and conc./ppm	T (°C)	Response (R_a/R_g) or (R_g/R_a)	Response time (s)/recovery time (s)	Long-term stability (days)	Detection limit	Ref.
AuPd/SnO_2 nanoparticles	H_2 100 ppm	150	72.8	Not reported	30	Not reported	58
AuPd/SnO_2 nanorods	H_2 100 ppm	175	46.4	19/302	35	Not reported	59
AuPd/ZnO NWs	NO_2 1 ppm	100	94.2	35/30	Not reported	Not reported	60
AuPd/In_2O_3 porous spheres	C_3H_9N 100 ppm	175	367.0	2/300	Stable for 30 days	300 ppb	61
AuPd/WO_3 hierarchical bundles	$C_4H_{10}O$ 50 ppm	200	91.0	8/12	20	1 ppm	62
AuPd/WO_3 nanorods	C_3H_6O 2 ppm	300	12.0	5/3	56	100 ppb	64
AuPd/SnO_2 nanosheets	C_3H_6O 2 ppm	250	6.6	4/6 (to 20 ppm acetone)	40	45 ppb	65
	HCHO 2 ppm	110	4.1	Not reported	40	30 ppb	
AuPd/WO_3 nanospheres	$C_4H_8O_2$ 10 ppm	250	400.0	8/4	30	100 ppb	69
PdAu/$W_{18}O_{49}$ nanowires	H_2S 50 ppm	100	55.5	10/9	56	Not reported	72
	CH_4 1000 ppm	320	7.8	25/15	56	Not reported	
PdRu/SnO_2 nanoclusters	C_3H_9N 100 ppm	230	78.3	10/81	15	1 ppm	74
AuPt/ZnO nanorods	H_2 250 ppm	130	157.4	115/not reported (RT)	Not reported	Not reported	75
AuPt/ZnO nanowires	H_2S 20 ppm	300	17.7	17/151	30	Not reported	76
AuPt/ZnO nanoflowers	C_7H_8 50 ppm	175	69.7	22/137	30	500 ppb	77
AuPt/In_2O_3 nanofibers	O_3 110 ppb	90	10.3	Not reported	30	20 ppb	78
	C_3H_6O 50 ppm	240	7.1	Not reported	30	500 ppb	
PtCu/WO_3/H_2O nanoplates	C_3H_6O 50 ppm	280	204.9	3/8	Not reported	10 ppb	79
$PtNi_3$/WO_3 nanoplates	HCOOH 100 ppm	220	591.0	3/not reported	60	500 ppb	80
AuPt/Carbon nanofibers	H_2 4 vol%	RT	48%	7/18	210	Not reported	81
Ni–Pt/CNF	H_2 100 ppm	RT	13%	32/72	Not reported	10 ppb	82
PtPd–WO_3 NFs	C_3H_6O 1 ppm	300	97.5	4.2/204	Not reported	1.07 ppb	83
PtRh–WO_3 NFs	C_3H_6O 1 ppm	350	104.0	4/176	Not reported	0.3 ppb	
PtPd/In_2O_3 nanoparticles	H_2 100 ppm	RT	29.8	58/200	30	Not reported	84
PdPt/ZnO nanorod clusters	H_2 1%	50	70%	5/76	Not reported	0.2 ppm	86
PdPt/SnO_2 NWs	NO_2 0.1 ppm	300	880.0	13/9	Not reported	Not reported	89
PtPd/Ru-implanted WS_2 nanosheets	C_3H_6O 50 ppm	20	4.2	77/48	Not reported	1 ppb	92
PdPt NOS-SnO_2	H_2 1000 ppm	50	75680	1/8	30	10 ppm	93
PtPd/SnO_2 multishell hollow microspheres	HCHO 1 ppm	190	867%	5/7	42	50 ppb	94
PtPd/SnO_2 nanosheets	CO 1 ppm	100	6.5	5/4	60	Not reported	95
	CH_4 500 ppm	320	3.1	5/4	60	Not reported	
PtRu/Flower-like WO_3	C_8H_{10} 100 ppm	170	261.0	2/329	14	1.97 ppm	97
Ag_6Au_1/In_2O_3 nanoclusters	HCHO 5 ppm	170	277.0	147/186	15	26 ppb	98
AgPd/ZnO nanoplates	H_2 500 ppm	400	78.0	2/13	28	800 ppb	99
AuAg/MWCNTs/WO_3	NO_2 1000 ppb	RT	1.995 ($\triangle R/R_a$) (%)	267/very slow recovery	95	45 ppb	100

Table 3 Summary of key properties of bimetallic systems used for enhancement of sensing performance of resistive gas sensors

Bimetallic system	Sensing material	Selectivity to gas	Long-term stability (days)	Ref.
AuPd	SnO_2 nanoparticles	H_2	30	58
	SnO_2 nanorods	H_2	35	59
	ZnO nanowires	NO_2	Not reported	60
	In_2O_3 porous spheres	C_3H_9N	30	61
	WO_3 hierarchical bundles	$C_4H_{10}O$	20	62
	WO_3 nanorods	C_3H_6O	35	64
	SnO_2 nanosheets	C_3H_6O, HCHO	40	65
	WO_3 nanospheres	$C_4H_8O_2$	30	69
	$W_{18}O_{49}$ nanowires	H_2S, CH_4	56	72
PdRu	SnO_2 nanoclusters	C_3H_9N	15	74
AuPt	ZnO nanorods	H_2	Not reported	75
	ZnO nanowires	H_2S	30	76
	ZnO nanoflowers	C_7H_8	30	77
	In_2O_3 nanofibers	O_3, C_3H_6O	30	78
	Carbon nanofibers	H_2	180	81
PtCu	WO_3/H_2O hollow sphere	C_3H_6O	Not reported	79
PtNi	WO_3 nanoplates	HCOOH	60	80
	Carbon nanofibers	H_2	Not reported	82
PtRh	WO_3 NFs	C_3H_6O	Not reported	83
PtPd	WO_3 NFs	C_3H_6O	Not reported	83
	In_2O_3 nanoparticles	H_2	30	84
	ZnO nanorod	H_2	Not reported	86
	SnO_2 NWs	NO_2	Not reported	89
	Ru-implanted WS_2 nanosheets	C_3H_6O	Not reported	92

Table 3 (*continued*)

Bimetallic system	Sensing material	Selectivity to gas	Long-term stability (days)	Ref.
	SnO_2	H_2	30	93
	SnO_2 multishell hollow microspheres	HCHO	42	94
	SnO_2 nanosheets	CO, CH_4	60	95
PtRu	Flower-like WO_3	C_8H_{10}	2	97
AuAg	In_2O_3 nanocluster	HCHO	15	98
	MWCNTs/WO_3	NO_2	95	100
AgPd	ZnO nanoplates	H_2	4	99

Finally, detection limits down to ppb levels have been reported for bimetal-decorated gas sensors, showing their potential for the development of highly sensitive and reliable gas sensors.

Table 3 summarizes the selectivity and long-term stability of various bimetal-decorated gas sensors. The selectivity ratio of $Au_{65}Pd_{35}$ bimetallic decoration for the SnO_2 gas sensor is 7.18, which is seven times higher than that of the pristine SnO_2 sensor at 150 °C.[58] While the optimal sensing temperature of the pristine ZnO sensor was 150 °C with a selectivity ratio of 3.15, AuPd bimetallic decoration decreased the sensing temperature to 100 °C and simultaneously increased the selectivity ratio to 14.95.[60] For the pristine In_2O_3 sensor, which operated optimally at temperatures above 250 °C, AuPd bimetallic decoration reduced the sensing temperature to 175 °C, achieving a high selectivity ratio of 10.00.[61] In addition, while the selectivity ratio of the pristine ZnO sensor was 1.00, PtAu bimetallic decoration increased the selectivity ratio to 14.70 at 130 °C.[75] Similarly, for the pristine ZnO sensor with an optimal sensing temperature of 200 °C, AuPt bimetallic decoration reduced the sensing temperature to 175 °C, resulting in a high selectivity ratio of 10.00.[77] Additionally, for a pristine WO_3 sensor with an optimal sensing temperature of 300 °C, $PtNi_3$ bimetallic decoration lowered the sensing temperature to 220 °C, achieving a selectivity ratio of 10.32.[80] In particular, for the NOS PdPt/SnO_2 sensor, the selectivity ratio was 1.87, while NOS Pd_2Pt/SnO_2 led to a dramatic increase in the selectivity ratio to 929.53 at 25 °C, achieved through an optimal Pd : Pt atomic loading ratio. These results underscore the effectiveness of bimetallic catalysts in improving both the selectivity and operating temperature of resistive gas sensors, highlighting their potential for high-performance applications.

The author contributions section should read as follows:

Author contributions

Ka Yoon Shin: conceptualization, writing – original draft; Yujin Kim: investigation, visualization; Ali Mirzaei: conceptualization, writing – original draft; Hyoun Woo Kim: supervision, validation; Sang Sub Kim: supervision, project administration, writing – review & editing.

The Royal Society of Chemistry apologises for these errors and any consequent inconvenience to authors and readers.

